Food Chemistry 316 (2020) 126303

Contents lists available at ScienceDirect

Food Chemistry

journal homepage: www.elsevier.com/locate/foodchem

*Exo*III and TdT dependent isothermal amplification (ETDA) colorimetric biosensor for ultra-sensitive detection of Hg^{2+}

XiangYang Li[a], ZaiHui Du[b], Shenghao Lin[b], JingJing Tian[b,c], HongTao Tian[d], WenTao Xu[b,c,*]

[a] Food Science and Engineering College, Beijing University of Agriculture, Beijing 102206, China
[b] College of Food Science and Nutritional Engineering, China Agricultural University, Beijing 100000, China
[c] Beijing Advanced Innovation Center for Food Nutrition and Human Health, China Agricultural University, Beijing 100000, China
[d] College of Food Science and Technology, Agricultural University of Hebei, Baoding 071000, China

ARTICLE INFO

Keywords:
*Exo*III
TdT
Hg^{2+}
Colorimetric biosensor
Double-amplification
Ultra-sensitivity

ABSTRACT

As the accumulation of mercury ions has a detrimental impact on human health, the design and development of a new type of biosensor that can rapidly, sensitively and selectively detect Hg^{2+} in aqueous solutions are essential. In this study, we have developed an exonuclease III (*Exo*III) and Terminal deoxynucleotidyl transferase (TdT) dependent isothermal amplification (ETDA) colorimetric biosensor. The template sequence is a hairpin where -NH_2 is labeled at the 3′-end and both termini are *T*-rich sequences. In the presence of Hg^{2+}, the template formed a blunt end, and the catalytic activity of *Exo*III was activated with cleavage of the -NH_2 at the 3′-end. TdT enzyme activity was initiated with the formation of a large number of G-rich nucleic acid sequences. G-rich sequences incubated with iron (III)-hemin mimicked peroxidase-like activity, catalyzing the oxidation of 3,3′,5,5′-tetramethylbenzidine (TMB) in the presence of H_2O_2. The biosensor constructed in this paper had a good linear range, 1–25 nmol/L. Its detection limit was 0.41 nmol/L (3σ), and recovery rates were between 100.5% and 103%. In conclusion, combined with the colorimetric biosensor and double enzyme cyclic amplification reaction, an ultra-sensitivity and strong specificity detection method was developed to detect Hg^{2+}. At the same time, this method also expands the detection method of Hg^{2+} available in the literature.

1. Introduction

In nature, mercury exists mainly in three forms, elemental mercury (Hg), organic mercury (alkyl mercury, phenyl mercury) and inorganic mercury (Hg^{+}, Hg^{2+}, and their complexes), and can be converted by biological and chemical means (Park & Zheng, 2012). With accelerating industrialization, increasing amounts of Hg^{2+} can easily be accumulated, due to the stability and persistence of Hg^{2+} (Renzoni, Zino, & Franchi, 1998). A highly toxic metal, Hg^{2+} is detrimental to environmental and human health even at low concentrations.

Traditional Hg^{2+} detection methods utilize various methodologies, including atomic absorption spectroscopy (AAS) (Ghaedi, Fathi, Shokrollahi, & Shajarat, 2006), atomic emission spectroscopy (AES) (Liu, Chen, et al., 2014), atomic fluorescence spectrometry (AFS) (Gao, Yang, Zheng, Hou, & Wu, 2010), inductively coupled plasma mass spectroscopy (ICP-MS) (Zhang et al., 2016), electrochemical analysis. Although these detection methods have high sensitivity and wide detection ranges, they are limited by their sophisticated apparatus requirements, cumbersome preparation processes, and problematic real-time detection (Mcghee, Loh, & Lu, 2017). In recent years, biochemical sensors using organic dyes, proteins, DNA (Hollenstein, Hipolito, Lam, Dietrich, & Perrin, 2010; Srinivasan, Subramanian, Murugan, Benelli, & Dinakaran, 2018) and thin films (Ren et al., 2018) have made great progress in the detection and analysis of Hg^{2+}, but there remain deficiencies, such as water solubility, sensitivity, stability, and selectivity. As a result, there is a need for a non-polluting, simple, rapid, highly sensitive, and highly specific method for trace Hg^{2+} detection in aqueous solutions.

Among the numerous methods for the detection of Hg^{2+}, colorimetric bioassays have an important role (Hai, Chen, Su, Xu, & Wang, 2018; Li, Dong, & Wang, 2009; Qi et al., 2018). They have many advantages of other techniques, such as sensitivity, quick response, and simple operation. The fundamental principle underlying these biosensors is the conversion of chemical signals of Hg^{2+} into optical signals.

Exonuclease III (*Exo*III) (Zhang, Yang, Lu, Wu, & Zhu, 2018) catalyzes cleavage duplex DNA from 3′-hydroxyl termini with stepwise removal of mononucleotides. Single-stranded DNA and 3′-protruding

* Corresponding author at: College of Food Science and Nutritional Engineering, China Agricultural University, Beijing 100000, China.
E-mail address: xuwentao@cau.edu.cn (W. Xu).

https://doi.org/10.1016/j.foodchem.2020.126303
Received 4 November 2018; Received in revised form 22 November 2019; Accepted 26 January 2020
Available online 28 January 2020

termini are resistant to *Exo*III cleavage, but the degree of resistance depends on the length of the extension, with extensions four bases or longer being completely resistant to cleavage (Xu, Cao, Zhang, & Zhang, 2012). RNase H, 3′-phosphatase and AP-endonuclease activities of *Exo* III have also been reported, and various biosensors have been designed utilizing these advantageous properties of *Exo* III (Jiang et al., 2018).

In 2004, Ono and Togashi (2004a,2004b) discovered that Hg^{2+} is able to coordinate with thymine nucleobases and that high-affinity structures (T-Hg^{2+}-T), which form between Hg^{2+} and the thymine-thymine base pairs, are more stable than the adenine–thymine (A-T) pairing (Ono & Togashi, 2004a,2004b; Sun, Du, He, & Jing, 2018). Xuan, Luo, and Hsing (2013) and Ren et al. (2016) demonstrated both blunt ends, formed by the mismatch between Hg^{2+} and thymidine, can exert the catalytic activity of *Exo*III.

Terminal deoxynucleotidyl transferase (TdT) is a unique DNA polymerase that can catalyze polymerization without the need for a template (Coleman, Hutton, De, & Bollum, 1975). The sequences produced by the TdT enzyme is random and non-specific. And the sequence produced is dependent largely on the constitution of the substrate deoxyribonucleoside triphosphate (dNTP) pool. Liu, Li et al. (2014) were first to demonstrate that the G-quadruplex structure could form in a guanine deoxyribonucleoside-rich pool via TdT polymerization.

In light of this knowledge, we designed an *Exo*III and TdT-dependent isothermal amplification (ETDA) colorimetric biosensor, exploiting the properties of T-Hg^{2+}-T, *Exo*III, and TdT, with T-Hg^{2+}-T as the identification component, *Exo*III and TdT as the amplifying components, and the product of TdT as a signal output element. The newly constructed biosensor is able not only to detect Hg^{2+} visually but also to detect trace amounts of Hg^{2+} in aqueous solutions due to the cycle amplification of the duel-enzyme.

2. Experimental

2.1. Chemicals

Mercury (II) nitrate ($Hg(NO_3)_2$) and sulfuric acid were obtained from Beijing Chemical Works (Beijing, China). dGTP and dATP were purchased from Takara Biotech (Dalian, China). SYBR® Gold Nucleic Acid Gel Stain and Thermo Scientific PageRuler Prestained Protein Ladder were purchased from Thermo Fisher Scientific (Waltham, USA). DM2000 marker was purchased from TransGen Biotech (Beijing, China). Exo III and TdT were purchased from New England BioLabs Inc. (Beverly, MA, USA). The agarose was purchased from Beijing Aoboxing Biotechnology Co., Ltd. (Beijing, China). Hemin, dimethyl sulfoxide, Ammonium persulfate (AP) and N, N, N', N'-Tetramethylethylenediamine (TEMED) were purchased from Sigma (St. Louis, MO, USA) and TMB chromogenic liquid was purchased from Shanghai Biyuntian Biotechnology Co., Ltd. (Shanghai, China) All reagents used in this work were of analytical grade.

All nucleic acids in this work were synthesized by Beijing RuiboXingke Biotech Co., Ltd. (Beijing, China) and purified by HPLC. The detail sequences of each nucleic acid are listed in Table 1. According to the manufacturer's specification sheet, a stock solution of 100 μM ssDNA was prepared by adding an appropriate volume of water to the aliquot provided. The nucleic acids were heated at 95 °C for 5 min and slowly cooled to room temperature until it formed a hairpin structure for subsequent experiments before use.

2.2. Instrumentation

A Millipore Mili-XQ system (Merck KGaA, Darmstadt, Germany), Thermo Scientific Varioskan Flash (Thermo Scientific, Waltham, USA), BioDoc-It Imaging System (UVP) and BioRad-S1000 PCR Instrument (American Bio-Rad Company, California, Hercules, USA) were also used.

2.3. Gel electrophoresis

The pre-experimental optimization of hairpin mismatch bases was analyzed using 20% PAGE. The gel consisted of 12.5 mL 40% acrylamide, 5 mL 5 × TBE buffer, 0.18 mL 10% AP (freshly prepared), 0.016 mL TEMED, and 7.3 mL H_2O. Then, samples of the experiment were run at 120 V for 1 h in 1 × TBE buffer and the gel was stained with SYBR® Gold Nucleic Acid Gel Stain, then the image was captured using BioDoc-It Imaging System.

The product TdT was analyzed on a 2% agarose gel (2 g agarose dissolved in 100 mL 1 × TAE buffer [50 × TAE buffer: 242 g Tris and 37.2 g $Na_2EDTA{\cdot}2H_2O$ were dissolved in 800 mL ddH2O, then 57.1 mL acetate was added, and finally was set to 1 L, pH8.0]). Ethidium bromide (1 μL, EB) was mixed with 2% agarose gel and the TdT product run at 130 V for 20 min in 1 × TAE buffer. The gel image was captured using a BioDoc-It Imaging System.

2.4. Detection of Hg^{2+}

Typically, *Exo*III reaction systems were comprised of 500 nmol/L hairpin sequences (see Table 1), 100 nmol/L Hg^{2+}, 1 × *Exo*III buffer, 1 U/μL *Exo*III made up the volume (50 μL). The reaction systems were incubated at 37 °C for 10 min and at 85 °C for another 10 min before 10 μL was added to 0.4 U/μL TdT, 1 × TdT buffer, 4 mmol/L dATP, 6 mmol/L dGTP and 0.25 mmol/L $CoCl_2$ in a total volume of 50 μL (TdT reaction systems). This TdT reaction was performed at 37 °C for 30 min and at 85 °C for 10 min. Next, 10 μL quantity of TdT reaction product, 80 μL 1 × Enzyme buffer (10 mmol/L Tris, 120 mmol/L NaCl, 10 mmol/L $MgCl_2{\cdot}6H_2O$, 10 mmol/L KCl, pH 8.4), and 10 μL hemin (10 mmol/L) were mixed and incubated at 37 °C for 30 min. And, 50 μL TMB was added and incubated at 37 °C for 5 min. Finally, 50 μL 2 mol/L H_2SO_4 was added to terminate the reaction (color reaction system). The absorbance was measured using either a microplate reader (450 nm) or the naked eye.

In order to simplify the experimental steps, we combined the ExoIII and TdT reaction systems (ETDA colorimetric biosensor) as follows: 500 nmol/L different hairpin sequences, 100 nmol/L Hg^{2+}, 1 × ExoIII buffer, 1 U/μL ExoIII, 0.4 U/μL TdT, 1 × TdT buffer, 4 mmol/L dATP, 6 mmol/L dGTP and 0.25 mmol/L $CoCl_2$, were combined to a total volume of 50 μL. This total reaction was performed at 37 °C for different times and at 85 °C for 10 min. Then, the color reaction systems were carried out using the same reaction system as above.

Table 1
Nucleic acid sequences.

Names	Nucleic acid sequences	Number of bases (nt)
Hairpin1	TTTTTTTTCGCATGCCAGATGCGGGATGGGCTGGCATGCGTTTTTTTT-NH_2	48
Hairpin2	TTTTTTCGCATGCCAGATGCGGGATGGGCTGGCATGCGTTTTTT-NH_2	44
Hairpin3	TTTTCGCATGCCAGATGCGGGATGGGCTGGCATGCGTTTT-NH_2	40

Notes: Hairpin is marked as -NH_2, and the hairpin is not marked as NH_2, in the following.

2.5. Determination of reaction conditions

In order to the obtained optimal performance of the sensor, we examined the reaction conditions including the base number of *T-T* mismatches in the hairpin DNA, TdT enzyme extension time, and dNTP composition. Optimization was carried out in the *Exo*III and TdT reaction system. Finally, we optimized the ETDA reaction time under optimal conditions.

2.6. The selectivity of the biosensor

To determine the selectivity of the newly biosensor, interfering several compounds and metal ions, including Hg_2Cl_2, CH_3Hg, Pb^{2+}, Zn^{2+}, Mg^{2+}, Ag^{+}, Cr^{3+}, Cd^{2+}, and Cu^{2+}. All test ion solutions were prepared at the same concentration of 1 μmol/L but added to the sensing system, individually.

2.7. Determination of spiked recovery

To evaluate the capability of the biosensor, we analyzed tap water from our laboratory. The water was spiked with different standard concentrations of Hg^{2+} (20 nM, 50 nM, and 100 nM). Otherwise, the procedures were the same as described above.

3. Results and discussion

3.1. Experimental principle and feasibility analysis

The construction of a Hg^{2+} functional nucleic acid colorimetric biosensor, based on *T*-Hg-*T* coordination and dual-enzyme amplification, is illustrated schematically in Scheme 1. The reaction is an *Exo*III- and TdT-dependent isothermal amplification (ETDA) reaction. In this experiment, the hairpin sequences were -NH_2 modified at a 3′-terminal and consisted of three sections, including a paired stem, unpaired loop, and *T*-rich nucleic sequences. In the absence of Hg^{2+}, the terminals did not match with one another, meaning the protruding 3′-end was resistant to *Exo*III. As the -NH_2 was modified at the 3′-end when the reaction system coexisted with the TdT enzyme, TdT enzyme activity was inhibited, preventing the polymerase product from being formed. In the presence of Hg^{2+}, based on Hg^{2+} mediated coordination of T-Hg^{2+}-T base pairs, the hairpin sequences formed complementary dsDNAs with a blunt 3′-end. *Exo*IIIIII catalyzed the stepwise removal of mononucleotides from the blunt 3′-ends, releasing the target Hg^{2+}, exposing the 3′-OH and activating the TdT enzyme, producing G-rich sequences in the appropriate ratio of dGTP and dATP. The extension product was a G-rich sequence with the peroxidase-like activity that catalyzed TMB to OXTMB with H_2O_2. As a consequence of the visible color changes, trace Hg^{2+} can be quantified.

The key underlying mechanism of the experiment is that hairpin sequences with -NH_2 at the 3′-end cannot be extended by TdT enzymes, in the absence of Hg^{2+}. It is only when Hg^{2+} is present that the hairpin sequences form blunt ends, which activate *Exo*III enzyme activity, expose 3′-OH ends, and activate TdT enzymes. The results are shown in Fig. 1. Firstly, the necessity of 3′ terminal labeled with -NH_2 was demonstrated. The results in Line 5 show that without -NH_2 modified hairpin sequences, TdT enzyme extension occurs. Results in Line 3 show that -NH_2 labeled hairpin sequences cannot be extended. Thus, we demonstrated that Hg^{2+} is an essential component for activating *Exo*III activity. Values in Lines 4 and 6 demonstrated that *Exo*III cleavage activity can only be activated in the presence of Hg^{2+}. These results prove the feasibility of the experimental approach, allowing us to optimize the experimental conditions.

3.2. Optimization of the number of mismatched bases

Since the formation of the hairpin blunt ends plays an important role in *Exo*III activation and Hg^{2+} detection, the number of mismatched bases was optimized. We added different hairpin sequences to the *Exo*III systems for experiments and observed the results of *Exo*III enzyme cleavage as shown in Fig. 2a. It is evident that the cleavage efficiency of Hairpin 2 was best. Hairpin 3 templates showed a non-specific cleavage in the absence of Hg^{2+}. This may be explained by the number of mismatched bases, which is less than four and/or weak interaction between each of bases, such that the non-complementary blunt ends of the hairpin are insufficient to inhibit *Exo*III activity. In the absence of Hg^{2+}, the templates of Hairpin 3 disappeared (Line 3). Hairpin 1 had a lower cleavage efficiency in the presence of 100 nmol/L Hg^{2+}. Considering the sensitivity of the biosensor, and due to the fact that mismatched bases require more Hg^{2+} to form a stable blunt end that triggers *Exo*III activity, a nucleic acid sequence with six mismatched bases was selected for subsequent experiments. However, results from the gel images showed that strips of cleaved products did not exist, possibly

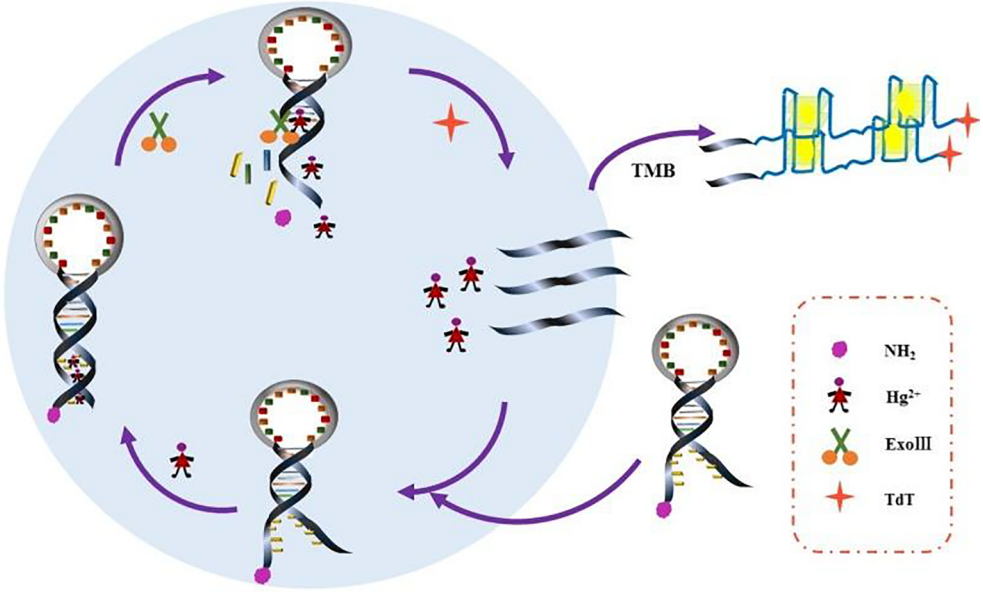

Scheme 1. The schematic of the detection of ETDA colorimetric biosensor.

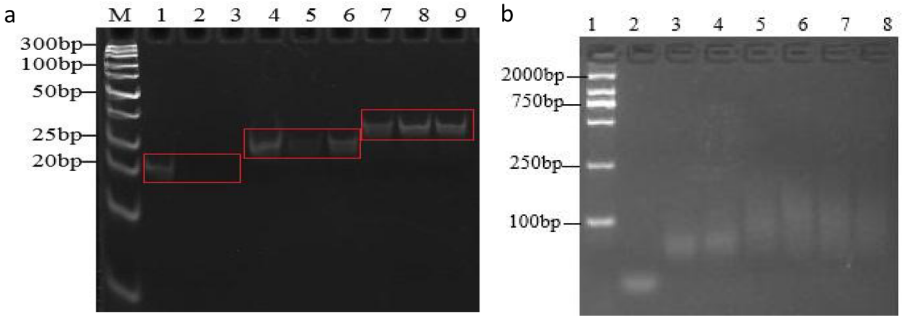

Fig. 1. Feasibility analysis of the experiment. Line1:Marker300;Line2:500 nmol/L hairpin2; Line3:500 nmol/L hairpin2 (without NH_2) + 0.4 U/μL TdT; Line4:500 nmol/L Hairpin2 + 100 nmol/L Hg^{2+} + 2.5 U/μL *Exo*III + 0.4 U/μL TdT;Line5:500 nmol/L Hairpin2 + 0.4 U/μL TdT;Line6:500 nmol/L Hairpin2 + 2.5 U/μL *Exo*III + 0.4 U/μL TdT Note: The sequences of hairpin2 and Hairpin2 are identical, but the hairpin2 is without -NH_2 modified hairpin sequences.

due to some other the characteristics of *Exo*III, such as RNase H, phosphatase and apurin/pyrimidine-endonuclease activities.

3.3. Optimization of TdT enzyme extension time

Considering the cost of the experiment, the templates used in the TdT reaction system without modified hairpin probes. Extension time for the TdT enzyme was found to affect detection time directly. In order to meet the requirements for quicker detection, we optimized TdT enzyme extension time, which is shown in Fig. 2b. It can be seen from Fig. 2b that length of extension product increased with time. However, when the extension time exceeded 30 min, the product no longer increased correspondingly. In order to minimize the detection time, an extension time of 30 min was selected.

3.4. Optimizing the ratio of dGTP and dATP for TdT enzyme

As a polymerase, TdT does not require a template and can be utilized to adjust a product according to different ratios of dNTPs in the system. We optimized the ratio of adenine and guanine to obtain a G-rich sequence that was more likely to form the G quadruplex with peroxidase-like activity. Results revealed when the ratio between adenine and guanine was 2:3, longer products and the best catalytic TMB effect could be achieved (Fig. 3). Although the ratio of adenine and guanine was higher at 1:1, the color reaction of TMB catalyzed by products was poor. This demonstrated that sequences formed at this ratio were less likely to form a G quadruplex with peroxidase-like activity. Therefore, we selected a ratio of 2:3 for TdT enzyme extension experiments.

3.5. Optimization of ETDA colorimetric biosensor

Since *Exo*III cannot cleave single-stranded products of the TdT enzyme, the two reaction systems can be combined to form a single isothermal cycle amplification reaction. The individual optimization results of the *Exo*III and TdT reaction systems were directly applied to the EDTA reaction system. And optimizated the time of EDTA reaction and shown in Fig. 4. The combined ETDA colorimetric biosensor did not affect the reaction results, thus allowing the process to be simplified. At 37 °C, the EDTA colorimetric biosensor was optimized at 50 min.

3.6. Detecting the property of Hg^{2+} biosensors

Under optimal conditions, the Hg^{2+} biosensor had a linear detection range from 1.0 nmol/L to 25 nmol/L. The absorbance maximum was at OD_{452}, where absorbance values were proportional to Hg^{2+} concentrations (Fig. 5a, $y = 0.028x + 0.157$, $R^2 = 0.997$). According to the calculation method, the formula for the minimum detection limit was:

minimum detection limit = the average blank absorbance + 3 σ (Standard deviation of 3 blank repeats), also known as the 3 σ principle. Similarly, according to the standard curve, the minimum concentration detection was 0.41 nmol/L. This suggests that the newly developed biosensor can be used to determine Hg^{2+} concentrations in water. Compared with alternatives, our method had greater sensitivity (Tan et al., 2017).

3.7. Specificity of the biosensor

The specificity of this biosensor was analyzed by comparing OD_{452} corresponding to Hg^{2+} concentration with that of interfering several

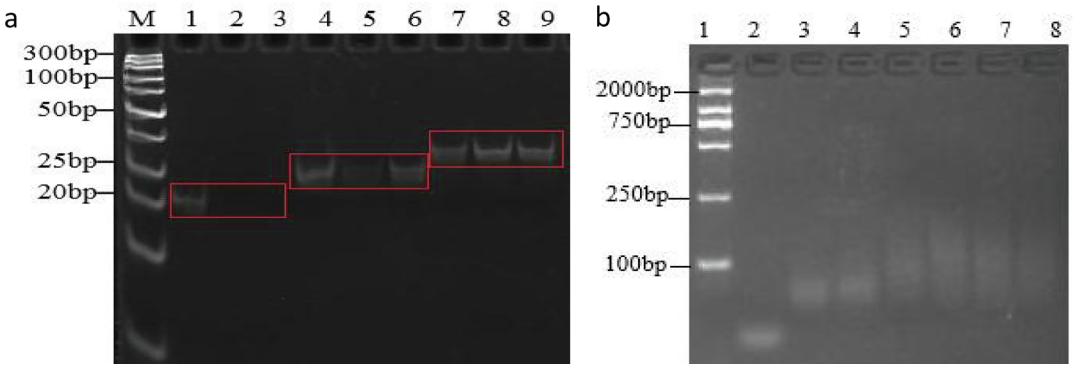

Fig. 2. (a) Optimization of the number of mismatched bases. Line M:Marker300; Line 1:500 nmol/L Hairpin 3; Line 2: 500 nmol/L Hairpin3 + 100 nmol/L Hg^{2+} + 2.5 U/uL *Exo*III;Line 3:500 nmol/L Hairpin3 + 2.5 U/uL *Exo*III;Line 4:500 nmol/L Hairpin2; Line 5:500 nmol/L Hairpin2 + 100 nmol/L Hg^{2+} + 2.5 U/uL *Exo*III; Line 6:500 nmol/L Hairpin2 + 2.5 U/uL *Exo*III; Line 7:500 nmol/L Hairpin1; Line 8:500 nmol/L Hairpin1 + 100 nmol/L Hg^{2+} + 2.5 U/uL *Exo*III; Line 9:500 nmol/L Hairpin1 + 2.5 U/uL *Exo*III; (b) Optimization of TdT enzyme extended time. Line 1: Marker2000; Line 2: 500 nmol/L hairpin2; Line 3: 500 nmol/L hairpin2 + 0.4 U/μL TdT 5 min; Line 4: 500 nmol/L hairpin2 + 0.4 U/μL TdT 10 min; Line 5: 500 nmol/L hairpin2 + 0.4 U/μL TdT 20 min; Line 6: 500 nmol/L hairpin2 + 0.4 U/μL TdT 30 min; Line 7: 500 nmol/L hairpin2 + 0.4 U/μL TdT 40 min; Line 8: 500 nmol/L hairpin2 + 0.4 U/μL TdT 1 h.

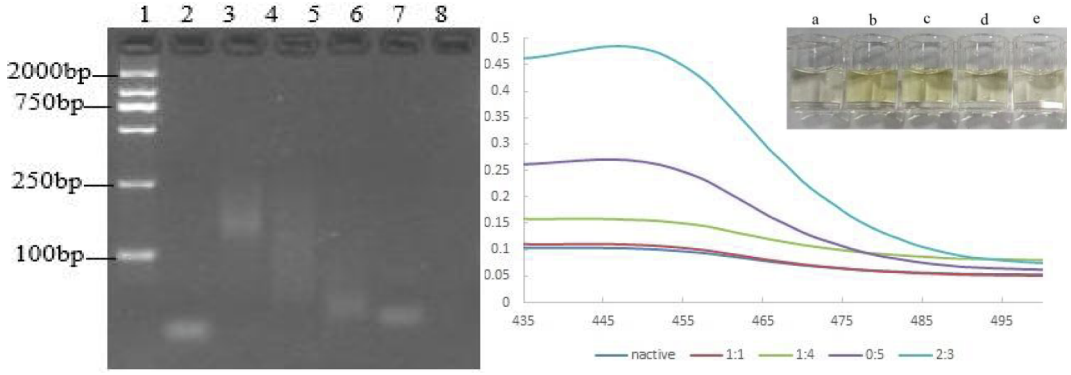

Fig. 3. TdT enzyme extension results of different substrate ratios. Line 1: Marker2000; Line 2:500 nmol/L hairpin2; Line 3:500 nmol/L hairpin2 + 0.4 U/μL TdT, dATP:dGTP = 1:1; Line 4:500 nmol/L hairpin2 + 0.4 U/μL TdT, dATP:dGTP = 2:3; Line 5:500 nmol/L hairpin2 + 0.4 U/μL TdT, dATP:dGTP = 1:4; Line 6:500 nmol/L hairpin2 + 0.4 U/μL TdT, 10 mmol/L dGTP. Illustrations a-e represent Line 2-Line 6 product coloration results.

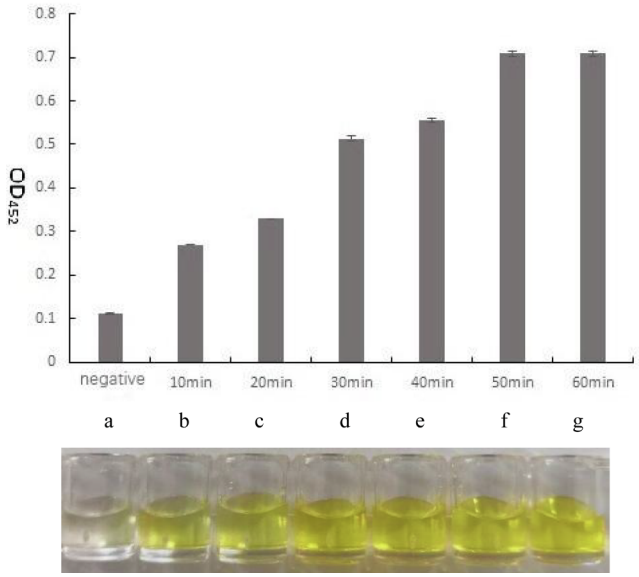

Fig. 4. Time optimization of ETDA colorimetric biosensorInsertion map: a is a negative sample, and b-g is a reaction diagram of the reaction system for 10–60 min.

compounds and metal ions, including Hg_2Cl_2, CH3Hg, Pb^{2+}, Zn^{2+}, Mg^{2+}, Ag^{+}, Cr^{3+}, Cd^{2+}, and Cu^{2+}. Fig. 5b shows that values for Hg^{2+} were significantly higher than other ions due to the specific binding of Hg^{2+} by thymine, resulting in *Exo*III exerting cleavage activity and TdT polymerase activity, which produces a large number of G-rich sequences to catalyze color development and, hence, obtain higher absorbance values. However, there is no specificity between other metal ions and thymine base-pair, thus absorbance values were lower. This showed that the ETDA colorimetric biosensor was selective for Hg^{2+}.

3.8. Determination of spiked recovery

In order to evaluate the practical value of this method, different concentrations of Hg^{2+} were added to the Hg^{2+}-free tap water to simulate naturally contaminated samples. Then, Hg^{2+} concentrations were determined using the newly developed ETDA colorimetric biosensor. The results are summarized in Table S1 and recoveries were in the range of 100.5% to 103%, indicating the assay provided acceptable analytical accuracy. Results from atomic fluorescence spectrometry (AFS) analysis are also shown in Fig. S1.

4. Conclusions

In conclusion, Hg^{2+}-mediated ssDNA can form a blunt-end hairpin structure, inducing *Exo*III and TdT enzyme activities, producing a number of G-rich sequences with the peroxidase-like activity that catalyzes coloration of H_2O_2 and TMB. A Hg^{2+} nucleic acid-sensitive detection method was constructed, creating an ETDA colorimetric biosensor. Constant temperature, simple operation, and short detection times mean that this ETDA colorimetric biosensor has potential value real-time in situ detection of Hg^{2+}. The detection limit of 0.41 nmol/L

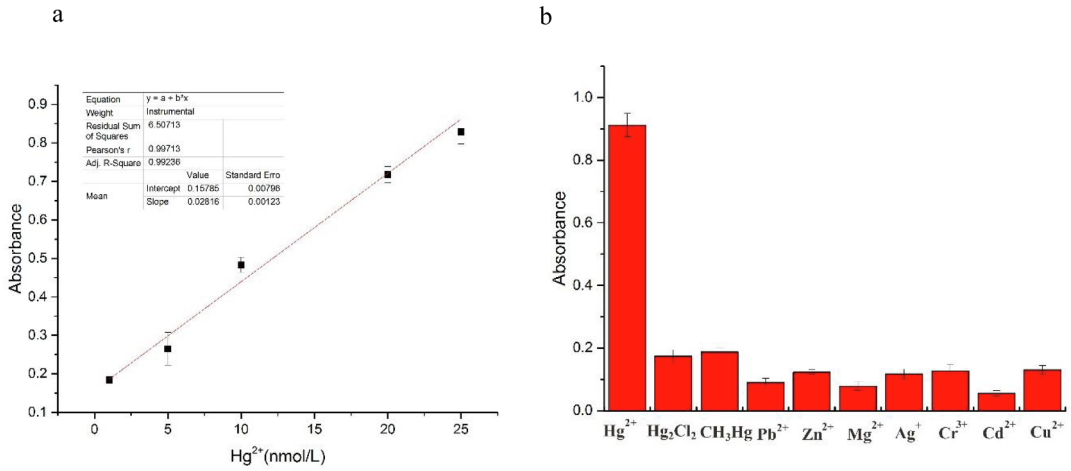

Fig. 5. (a) Linearity and sensitivity of the ETDA colorimetric biosensor; (b) Selectivity of ETDA colorimetric biosensor for Hg^{2+} determination.

meets the sensitivity required by the United States Environmental Protection Agency (US EPA). Compared with existing Hg^{2+} biosensors, the ETDA colorimetric biosensor designed in this study offers the following advantages: (1) it relies on mismatches with T-Hg^{2+}-T, making the sensor highly specific; (2) dual-enzyme amplification of *Exo*III and TdT makes the detection method particularly sensitive and reliable; and (3) operation of the experiment is simple, independent of large-scale equipment, and the detection of actual samples is equally straightforward.

CRediT authorship contribution statement

XiangYang Li: Methodology, Project administration, Writing - review & editing. **ZaiHui Du:** Formal analysis, Writing - original draft. **Shenghao Lin:** Data curation, Software. **JingJing Tian:** Investigation, Validation. **HongTao Tian:** Supervision. **WenTao Xu:** Conceptualization, Funding acquisition, Resources.

Declaration of Competing Interest

The authors declare that they have no known competing financial interests or personal relationships that could have appeared to influence the work reported in this paper.

Acknowledgements

This work was financially supported by the Natural Science Foundation of China (Grant No.31671922) and Beijing Municipal Education Commission Research Project (KM201910020002).

Appendix A. Supplementary data

Supplementary data to this article can be found online at https://doi.org/10.1016/j.foodchem.2020.126303.

References

Coleman, M. S., Hutton, J. J., De, S. P., & Bollum, F. J. (1975). Terminal deoxyribonucleotidyl transferase in human leukemia. *Proceedings of the National Academy of Sciences of the United States of America, 62*(2), 367.

Gao, Y., Yang, W., Zheng, C., Hou, X., & Wu, L. (2010). On-line preconcentration and in situ photochemical vapor generation in coiled reactor for speciation analysis of mercury and methylmercury by atomic fluorescence spectrometry. *Journal of Analytical Atomic Spectrometry, 26*(1), 126–132.

Ghaedi, M., Fathi, M. R., Shokrollahi, A., & Shajarat, F. (2006). Highly selective and sensitive preconcentration of mercury ion and determination by cold vapor atomic absorption spectroscopy. *Analytical Letters, 39*(6), 1171–1185.

Hai, J., Chen, F., Su, J., Xu, F., & Wang, B. (2018). Porous wood members-based amplified colorimetric sensor for Hg2+ detection through Hg2+-triggered methylene blue reduction reactions. *Analytical Chemistry, 90*(7), 4909–4915.

Hollenstein, M., Hipolito, C., Lam, C., Dietrich, D., & Perrin, D. M. (2010). A highly selective DNAzyme sensor for mercuric ions. *Angewandte Chemie International Edition, 47*(23), 4239.

Jiang, X., Liu, H., Khusbu, F. Y., Ma, C., Ping, A., Zhang, Q., ... Chen, M. (2018). Label-free detection of exonuclease III activity and its inhibition based on DNA hairpin probe. *Analytical Biochemistry, 555*, 55–58.

Li, T., Dong, S., & Wang, E. (2009). Label-free colorimetric detection of aqueous mercury ion (Hg2+) using Hg2+-modulated G-quadruplex-based DNAzymes. *Analytical Chemistry, 81*(6), 2144–2149.

Liu, J., Chen, L., Chen, J., Ge, C., Fang, Z., Wang, L., ... Zeng, L. (2014). An autonomous T-rich DNA machine based lateral flow biosensor for amplified visual detection of mercury ions. *Analytical Methods, 6*(7), 2024–2027.

Liu, Z., Li, W., Nie, Z., Peng, F., Huang, Y., & Yao, S. (2014). Randomly arrayed G-quadruplexes for label-free and real-time assay of enzyme activity. *Chemical Communications, 50*(52), 6875–6878.

Mcghee, C. E., Loh, K. Y., & Lu, Y. (2017). DNAzyme sensors for detection of metal ions in the environment and imaging them in living cells. *Current Opinion in Biotechnology, 45*, 191.

Ono, A., & Togashi, H. (2004a). Highly selective oligonucleotide-based sensor for mercury (II) in aqueous solutions. *Angewandte Chemie International Edition, 43*(33), 4300–4302.

Ono, A., & Togashi, H. (2004b). Highly selective oligonucleotide-based sensor for mercury (II) in aqueous solutions. *Angewandte Chemie, 116*(33), 4400–4402.

Park, J. D., & Zheng, W. (2012). Human exposure and health effects of inorganic and elemental mercury. *Journal of Preventive Medicine & Public Health, 45*(6), 344–352.

Qi, Y., Zhao, J., Weng, G., Li, J., Zhu, J., & Zhao, J. (2018). Modification-free colorimetric and visual detection of Hg2+ based on the etching from core-shell structural Au-Ag nanorods to nanorices. *Sensors and Actuators B: Chemical, 267*, 181–190.

Ren, M., Wang, Y., Ding, S., Yang, L., Sun, Q., & Zhang, L. (2018). Development of a new diffusive gradients in thin films (DGT) method for the simultaneous measurement of CH3Hg+ and Hg2+. *New Journal of Chemistry*.

Ren, W., Zhang, Y., Chen, H. G., Gao, Z. F., Li, N. B., & Luo, H. Q. (2016). Ultrasensitive label-free resonance rayleigh scattering aptasensor for Hg2+ using Hg2+-triggered exonuclease III-assisted target recycling and growth of G-wires for signal amplification. *Analytical Chemistry, 88*(2), 1385–1390.

Renzoni, A., Zino, F., & Franchi, E. (1998). Mercury levels along the food chain and risk for exposed populations. *Environmental Research, 77*(2), 68.

Srinivasan, K., Subramanian, K., Murugan, K., Benelli, G., & Dinakaran, K. (2018). Fluorescence quenching of MoS2 nanosheets/DNA/silicon dot nanoassembly: Effective and rapid detection of Hg2+ ions in aqueous solution. *Environmental Science & Pollution Research International*, 1–10.

Sun, Z., Du, J., He, K., & Jing, C. (2018). T-Hg2+-T-based satellite structured surface enhanced Raman scattering sensor for Hg2+ detection. *Journal Of Raman Spectroscopy*.

Tan, L., Chen, Z., Zhang, C., Wei, X., Lou, T., & Zhao, Y. (2017). Colorimetric detection of Hg2+ based on the growth of aptamer-coated AuNPs: The effect of prolonging aptamer strands. *Small, 13*(14), 1603370.

Xu, Q., Cao, A., Zhang, L. F., & Zhang, C. Y. (2012). Rapid and label-free monitoring of exonuclease III-assisted target recycling amplification. *Analytical Chemistry, 84*(24), 10845.

Xuan, F., Luo, X., & Hsing, I. M. (2013). Conformation-dependent exonuclease III activity mediated by metal ions reshuffling on thymine-rich DNA duplexes for an ultrasensitive electrochemical method for Hg2+ detection. *Analytical Chemistry, 85*(9), 4586–4593.

Zhang, K., Yang, L., Lu, F., Wu, X., & Zhu, J. J. (2018). Cancer diagnosis: A universal upconversion sensing platform for the sensitive detection of tumour-related ncRNA through an Exo III-assisted cycling amplification strategy (Small 10/2018). *Small, 14*(10), 1870044.

Zhang, S., Luo, H., Zhang, Y., Li, X., Liu, J., Xu, Q., & Wang, Z. (2016). In situ rapid magnetic solid-phase extraction coupled with HPLC-ICP-MS for mercury speciation in environmental water. *Microchemical Journal, 126*, 25–31.